

# Efficient broadband sum and difference frequency generation with a single chirped quasi-phase-matching crystal

A. A. Rangelov

*Department of Physics, Sofia University, James Bourchier 5 blvd., 1164 Sofia, Bulgaria*

(Dated: August 6, 2017)

We propose an efficient broadband frequency generation technique for two collinear optical parametric processes  $\omega_3 = \omega_1 + \omega_2$  and  $\omega_4 = \omega_1 - \omega_2$ . It exploits chirped quasi-phase-matched gratings, which in the undepleted pump approximation regime perform population transfer that is analogous to adiabatic population transfer in a three-state “vee” quantum system. The energy of the input fields is transferred adiabatically either into  $\omega_3$  or  $\omega_4$  field, depending on which of the two phase matchings occurs first by the local modulation period in the crystal. One can switch the output between  $\omega_3$  and  $\omega_4$  by inverting the direction of the local modulation sweep, which corresponds to a rotation of the crystal by angle  $\pi$ .

PACS numbers: 42.65.-k, 42.65.Ky, 42.79.Nv, 42.25.Kb

## I. INTRODUCTION

Sum frequency generation (SFG) and difference frequency generation (DFG) occur, when two input beams generate another beam with the sum (SFG) or the difference (DFG) of the optical frequencies of the input beams [1–3]. In order to be efficient these processes traditionally require phase matching [1–3], which is usually difficult to achieve simultaneously for SFG and DFG [1–3].

Recently Suchowski *et al.* [4–6] used an aperiodically poled quasi-phase-matching (QPM) crystal to achieve both high efficiency and large bandwidth in SFG and DFG in the regime of undepleted pump approximation. Their approach was based on ideas from rapid adiabatic passage in two-state quantum systems [7–9].

In this paper, this method is further extended to realize a potentially highly efficient broadband SFG and DFG with a single crystal. This is achieved by treating the two simultaneous collinear second-order parametric processes  $\omega_3 = \omega_1 + \omega_2$  and  $\omega_4 = \omega_1 - \omega_2$  in analogy to coherent population transfer in three-state “vee” quantum systems. The analogy to level crossings in atomic systems [7–9] ensues from the linearly chirped QPM gratings [10–12] that we use to this end.

## II. BACKGROUND

The SFG and DFG processes for a QPM crystal with susceptibility  $\chi^{(2)}$  and local modulation period  $\Lambda(z)$  are described by two sets of nonlinear differential equations [1–3]

$$i\partial_z E_1 = \Omega_1 E_2^* E_3 e^{-i\Delta_1 z}, \quad (1a)$$

$$i\partial_z E_2 = \Omega_2 E_1^* E_3 e^{-i\Delta_1 z}, \quad (1b)$$

$$i\partial_z E_3 = \Omega_3 E_1 E_2 e^{i\Delta_1 z}. \quad (1c)$$

$$i\partial_z E_1 = \Omega_1 E_2^* E_4 e^{-i\Delta_2 z}, \quad (2a)$$

$$i\partial_z E_2 = \Omega_2 E_1^* E_4 e^{-i\Delta_2 z}, \quad (2b)$$

$$i\partial_z E_4 = \Omega_4 E_1 E_2 e^{i\Delta_2 z}, \quad (2c)$$

where  $z$  is the position along the propagation axis,  $c$  is the speed of light in vacuum, and  $E_j$ ,  $\omega_j$  and  $n_j$  are the electric field, the frequency and the refractive index of the  $j$ -th laser beam, respectively. The coupling coefficients are

$$\Omega_j = \chi^{(2)} \omega_j / 4cn_j \quad (j = 1, 2, 3, 4), \quad (3)$$

while the phase mismatches for SFG and DFG processes are

$$\Delta_1 = \omega_1 n_1 / c + \omega_2 n_2 / c - \omega_3 n_3 / c + 2\pi / \Lambda, \quad (4a)$$

$$\Delta_2 = n_1 \omega_1 / c + \omega_2 n_2 / c - \omega_4 n_4 / c + 2\pi / \Lambda. \quad (4b)$$

We combine Eqs. (1) with Eqs. (2) to write a system of differential equations that describes the two simultaneously running processes

$$i\partial_z E_1 = \Omega_1 (E_1^* E_2 e^{-i\Delta_1 z} + E_1^* E_4 e^{-i\Delta_2 z}), \quad (5a)$$

$$i\partial_z E_2 = \Omega_2 (E_1^* E_3 e^{-i\Delta_1 z} + E_1^* E_4 e^{-i\Delta_2 z}), \quad (5b)$$

$$i\partial_z E_3 = \Omega_3 E_1 E_2 e^{i\Delta_1 z}, \quad (5c)$$

$$i\partial_z E_4 = \Omega_4 E_1 E_2 e^{i\Delta_2 z}. \quad (5d)$$

## III. ADIABATIC EVOLUTION OF SFG AND DFG IN UNDEPLETED PUMP APPROXIMATION

The coupled nonlinear equations (5) can be linearized if we assume that the incident pump field  $E_1$  is much stronger than the other fields. In this case its amplitude is nearly constant (undepleted) during evolution and as a result Eqs. (5) are reduced to a system of three linear

equations,

$$i\partial_z \mathbf{A}(z) = \mathbf{H}(z)\mathbf{A}(z), \quad (6a)$$

$$\mathbf{H} = \begin{bmatrix} \Delta_1 & \Omega_P & 0 \\ \Omega_P & 0 & \Omega_S \\ 0 & \Omega_S & \Delta_2 \end{bmatrix}, \quad (6b)$$

with

$$\Omega_P = E_1 \sqrt{\Omega_2 \Omega_3}, \quad (7a)$$

$$\Omega_S = E_1 \sqrt{\Omega_2 \Omega_4}, \quad (7b)$$

$$\mathbf{A}(z) = [A_3(z), A_2(z), A_4(z)]^T, \quad (7c)$$

$$A_2 = E_2 / \sqrt{\Omega_2}, \quad (7d)$$

$$A_3 = E_3 e^{-i\Delta_1 z} / \sqrt{\Omega_3}, \quad (7e)$$

$$A_4 = E_4 e^{-i\Delta_2 z} / \sqrt{\Omega_4}. \quad (7f)$$

Upon the substitution  $z \rightarrow t$ , Eq. (6) becomes identical to the time-dependent Schrödinger equation for a three-state quantum system in the rotating-wave approximation; the vector  $\mathbf{A}(z)$  and the driving matrix  $\mathbf{H}$  correspond to the quantum state vector and the Hamiltonian, respectively. The diagonal terms of the matrix  $\mathbf{H}$ ,  $\Delta_1$ , 0 and  $\Delta_2$ , correspond to the detunings while the off-diagonal terms,  $\Omega_P$  and  $\Omega_S$ , correspond to pump and Stokes Rabi frequencies. We note that the quantity  $|\mathbf{A}(z)|^2 = |A_3(z)|^2 + |A_2(z)|^2 + |A_4(z)|^2$  is conserved, analogously to the total population in a coherently driven quantum system. If the energy is initially in the input electric field with frequency  $\omega_2$

$$\mathbf{A} = [0, A_2, 0], \quad (8)$$

then the three linear equations (6) will form a “vee” pattern analogously to the “vee” configuration of a three-state quantum system (see Fig. 1). We assume that phase mismatches either increase (sign +) or decrease (sign -) linearly along  $z$

$$\Delta_1 = \delta_1 \pm \alpha^2 z, \quad (9a)$$

$$\Delta_2 = \delta_2 \pm \alpha^2 z, \quad (9b)$$

which can be achieved, for example, by varying the local modulation period  $\Lambda(z)$ . For the sake of generality, we take hereafter  $\alpha$  as the unit of coupling and  $1/\alpha$  as the unit of length. Therefore the three eigenvalues of  $\mathbf{H}$  cross at two different distances  $z_m$  ( $m = 1, 2$ ), thereby creating a crossing pattern in analogy with two parallel energies crossed by a third, tilted energy in quantum physics [13]. This crossing pattern can be easily examined by the famous Landau-Zener-Stückelberg-Majorana (LZSM) model [14–17], which is the most popular tool for estimating the transition probability between two states of crossing energies. This model assumes a constant interaction of infinite duration and linearly evolving energies. Owing to some mathematical subtleties, the LZSM model often provides more accurate results than anticipated. Its popularity is further promoted by the

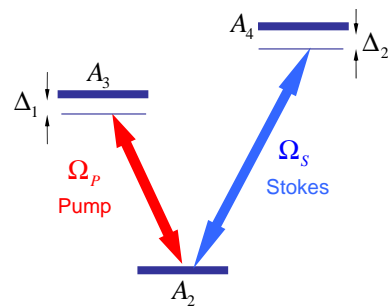


FIG. 1: (Color online) The “vee” linkage pattern for the linearized system (6), treated in analogy to the “vee” configuration of a three-state quantum system.

extreme simplicity of the transition probability expressions it derives. The LZSM model has been extended to three and more levels by a number of authors. In the Demkov-Osherov (DO) model [18, 19], a single tilted energy crosses a set of  $N$  parallel energies. Our case, cf. Eqs. (6) and Eqs. (9), matches the DO model with two parallel energies crossed by single tilted energy, as shown in the top frames of Fig. 2.

The proposed SFG and DFG are illustrated in Fig. 2. The top frames plot the eigenvalues of  $\mathbf{H}$  ( $\varepsilon_1$ ,  $\varepsilon_2$  and  $\varepsilon_3$ ) vs  $z$ . Initially only the  $\omega_2$  field is present (see Eq.(8)). If the evolution is adiabatic then there are two possible paths that the system can follow (left and right frames). If the phase match for the  $\omega_3$  generation process occurs first (left frames of Fig. 2), then the energy is passed into the  $\omega_3$  field. If instead first we observe the phase match for the  $\omega_4$  generation process (right frames of Fig. 1), then efficient energy transfer to the  $\omega_4$  field takes place.

The bottom frames of Fig. 2 show the evolution of the normalized light intensities for the three possible frequencies  $\omega_2$ ,  $\omega_3$  and  $\omega_4$ . The left and the right scenarios extend the single-step adiabatic passage scenario for either SFG or DFG [4–6].

In the beginning and at the end each eigenfrequency  $\varepsilon_i(z)$ ,  $i = 1, 2, 3$ , coincides with one of the intrinsic diagonal terms of  $\mathbf{H}$ , while in between it is a superposition of these terms. In the adiabatic limit, the system follows the eigenstate of  $\mathbf{H}(z)$ , which asymptotically coincides with the initial state of the system. Correspondingly, the frequency of the system at any instant of  $z$  is the frequency of this state, i.e. for the initial condition (8)  $\varepsilon_1(z)$ . However, the composition of  $\varepsilon_1(z)$  is different for DFG and SFG because the order of the crossings differ. Reordering the crossings can be easily done by  $z$  reversal. Hence one can achieve either SFG or DFG with a single chirped QPM crystal just by rotating it on an angle  $\pi$ .

Next we turn our attention to the conditions needed for adiabatic evolution in the two distinct cases of SFG and DFG. By applying the LZSM model [14–17]

$$p = 1 - \exp(-2\pi\Omega^2/\alpha^2), \quad (10)$$

we find that to obtain transition probability larger than  $1 - \epsilon$  we must satisfy the following conditions at each

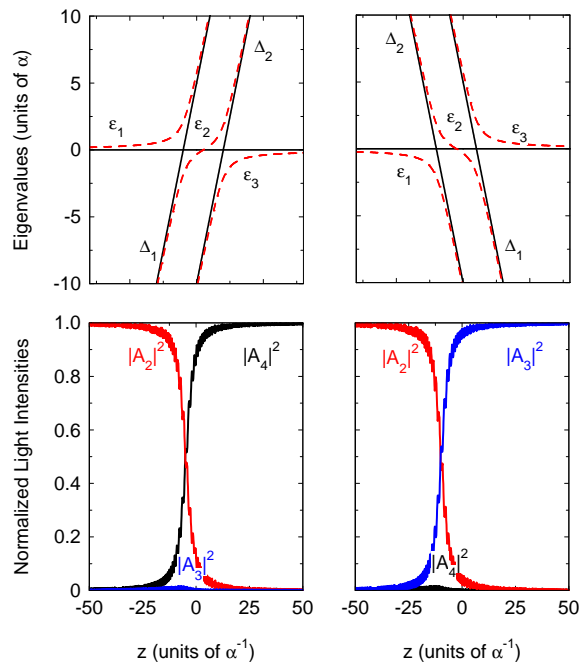


FIG. 2: (Color online) Schematic evolution of frequency generation obtained by numerical integration of Eqs. (6) for  $\delta_1 = -10\alpha$ ,  $\delta_2 = 5\alpha$  and  $\Omega_p = \Omega_s = 2\alpha$ . Left frames: SFG with increasing phase mismatches. Right frames: DFG with decreasing phase mismatches. Top frames: Diagonal elements (solid lines) and eigenvalues (dashed lines) of the driving matrix  $\mathbf{H}$  of Eq. (6). Bottom frames: normalized light intensities. The sign difference in Eq. (9) between the left and the right frames corresponds to  $z$  reversal (rotation of the crystal by angle  $\pi$ ).

crossing

$$\frac{\Omega}{\alpha} > \sqrt{\frac{\ln(1/\epsilon)}{2\pi}}, \quad (11)$$

where  $\Omega = \Omega_p$  for SFG and  $\Omega = \Omega_S$  for DFG. One can

readily verify that the conditions are satisfied for the parameters used in Fig. 2.

As was shown earlier [4–6] in analogy with atomic physics, adiabatic implementation of both SFG and DFG leads to robustness of the adiabatic approach against variations of the parameters such as propagation distance, couplings and initial (final) phase mismatches. Our approach shares the same robustness as previously proposed adiabatic schemes, which includes stability to variation of crystal temperature, wavelengths of the input electric fields, crystal length and angle of incidence.

#### IV. CONCLUSION

We have used the analogy between the time-dependent Schrödinger equation and the SFG/DFG equations in the undepleted pump approximation regime to propose an efficient broadband SFG/DFG technique realized with a single crystal. A local modulation period sweep along the light propagation creates crossings in the phase matching between different parametric processes, which in combination with adiabatic evolution conditions allow for both efficient and robust SFG and DFG for the input frequencies. Chirped adiabatic QPM gratings offer robustness against variations of the parameters of both the crystal and the electric fields, which include the crystal temperature, the wavelengths of the input electric fields, the crystal length and the angle of incidence.

The present work can be viewed as a generalization of the idea of Suchowski *et al.* [6], however applied simultaneously for SFG and DFG in a single crystal.

#### Acknowledgments

This work is supported by the European network FASTQUAST and the Bulgarian NSF grants D002-90/08 and DMU02-19/09.

- 
- [1] R. W. Boyd, *Nonlinear Optics*, Academic, New York, 2007.
  - [2] B. E. A. Saleh and M. C. Teich, *Fundamentals of Photonics*, John Wiley & Sons, New Jersey, 2007.
  - [3] A. Yariv and P. Yeh, *Photonics: Optical Electronics in Modern Communications*, Oxford University Press, New York, 2007.
  - [4] H. Suchowski, D. Oron, A. Arie, and Y. Silberberg, *Phys. Rev. A* 78 (2008) 063821.
  - [5] H. Suchowski, V. Prabhudesai, D. Oron, A. Arie, and Y. Silberberg, *Opt. Express* 17 (2009) 12731.
  - [6] H. Suchowski, B. D. Bruner, A. Ganany-Padowicz, I. Juwiler, A. Arie, and Y. Silberberg, *Appl. Phys. B* 105 (2011) 697.
  - [7] L. Allen, J. H. Eberly, *Optical Resonance and Two-Level Atoms*, Dover, New York, 1987.
  - [8] N. V. Vitanov, T. Halfmann, B. W. Shore, and K. Bergmann, *Annu. Rev. Phys. Chem.* 52 (2001) 763.
  - [9] B. W. Shore, *Acta Phys. Slovaca* 58 (2008) 243.
  - [10] M. Charbonneau-Lefort, B. Afeyan, and M. M. Fejer, *J. Opt. Soc. Am. B* 25 (2008) 463.
  - [11] M. Charbonneau-Lefort, M. M. Fejer, and B. Afeyan, *Opt. Lett.* 30 (2005) 634.
  - [12] M. A. Arbore, O. Marco, and M. M. Fejer, *Opt. Lett.* 22 (1997) 865.
  - [13] A. A. Rangelov, J. Piilo, and N. V. Vitanov, *Phys. Rev. A* 72 (2005) 053404.
  - [14] L. D. Landau, *Physik Z. Sowjetunion* 2 (1932) 46.
  - [15] C. Zener, *Proc. R. Soc. Lond. Ser. A* 137 (1932) 696.
  - [16] E. C. G. Stückelberg, *Helv. Phys. Acta* 5 (1932) 369.
  - [17] E. Majorana, *Nuovo Cimento* 9 (1932) 43.
  - [18] Y. N. Demkov and V. I. Osherov, *Zh. Eksp. Teor. Fiz.*

53 (1967) 1589 [Sov. Phys. JETP 26 (1968) 916].

[19] Y. Kayanuma and S. Fukuchi, J. Phys. B 18 (1985) 4089.